The Design of Stretchable and Self-Healing Gel Electrolytes via Fully-Zwitterionic Polymer Networks in Solvate Ionic Liquids for Li-based Batteries

*Anthony J. D'Angelo and Matthew J. Panzer**

Department of Chemical & Biological Engineering, Tufts University, 4 Colby Street, Medford, MA 02155

Corresponding Author:

*Email: matthew.panzer@tufts.edu

Abstract

An emerging class of ion-dense electrolytes consisting of complexed lithium cations and weakly basic anions, known as solvate ionic liquids, possess many desirable attributes for lithium-based electrochemical energy storage. In this study, a series of fully-zwitterionic (f-ZI) polymer scaffold-supported solvate ionogels are synthesized via UV-initiated free-radical (co)polymerization of two zwitterionic monomers, 2-methacryloyloxyethyl phosphorylcholine (MPC) and sulfobetaine vinylimidazole (SBVI), *in situ* within the solvate ionic liquid [Li(G4)][TFSI], which is prepared from an equimolar mixture of lithium bis(trifluoromethylsulfonyl)imide (LiTFSI) and tetraglyme (G4). Systematically varying the MPC:SBVI molar ratio within the f-ZI polymer network enables one to widely tune the mechanical properties of the poly(MPC-co-SBVI)-supported solvate ionogel composites. For a fixed polymer content of 20 mol%, gel compressive elastic modulus values are observed to span two orders of magnitude, from 23 kPa to 7.3 MPa, while the room temperature ionic conductivity values remain fairly unchanged (between 0.48 mS cm^{-1} and 0.70 mS cm^{-1}). MPC-rich copolymer formulations lead to solvate ionogels that exhibit substantial

plastic deformation, exceeding 200% tensile strain prior to failure, and Li-ion transference numbers as high as 0.60, which represents a five-fold increase compared to the neat solvate ionic liquid electrolyte. A 20 mol% poly(MPC-co-SBVI)-supported solvate ionogel having a 3:1 MPC:SBVI molar ratio successfully enables the galvanostatic cycling of a lithium-ion battery prototype for 100 cycles at a rate of C/2, demonstrating the viability of these safer gel electrolytes for lithium-based energy storage devices.

Introduction

Ionic liquids (ILs), or room temperature molten salts, have garnered increasing interest as potential electrolyte materials for Li-based batteries due to their unique properties of moderate room temperature ionic conductivity (1–10 mS cm^{-1}), high electrochemical stability (3–5 V window), and enhanced safety due to a negligible vapor pressure.[1-2] Traditional IL-based electrolytes for lithium batteries are realized by dissolution of a lithium salt into an IL, which results in a marked increase in solution viscosity at practical Li^+ concentrations (0.1–1 M).[3] Li salt-IL solutions typically exhibit room temperature ionic conductivities in the range of 0.1–1 mS cm^{-1} with a Li^+ transference number (t_{Li^+}) of ~0.3, owing to the nature of ternary ionic species systems.[4] Recently, an emergent IL subclass of ion-dense, lithium-containing electrolytes is actively being investigated within the research community, namely, *solvate* ionic liquids (SILs).[5-8] SILs demonstrate comparable benefits of traditional ILs, such as ultralow vapor pressure and nonflammability, yet are comprised of readily-available/low cost reagents (*e.g.* lithium salt + oligoether ligand) that suggest greater viability of these electrolytes for commercialization. SILs display properties comparable to ILs due to the formation of a complex ion (either cation or anion) from the combination of a salt and a strongly coordinating ligand.[7] Pappenfus *et al*. reported an

early example of a SIL via an equimolar combination of lithium bis(trifluoromethylsulfonyl)imide (LiTFSI) with the organic ligand tetra(ethylene glycol) dimethyl ether (tetraglyme, G4) to form [Li(G4)][TFSI].[5] Although there is a relatively high concentration of lithium salt in [Li(G4)][TFSI] (*i.e.* 2.8 M), the solvated cation structure of this SIL prevents the clustering of anions around bare Li^+ cations that tends to increase the viscosity of traditional IL/lithium salt solutions, allowing [Li(G4)][TFSI] to exhibit a room temperature ionic conductivity of ~1 mS cm^{-1}.[5]

The emergence of highly flexible and stretchable electronics has sparked the imaginations of many in recent years. Flexible energy storage devices could find a myriad of applications in the advancement of 'smart' textiles, electronic skins, implantable devices, large displays, and mobile devices.[9] In order to build a stable device, a flexible/stretchable battery must be able to withstand the mechanical deformation requirements of the intended application while still retaining its electrochemical performance. One approach to realize a flexible/stretchable battery electrolyte that leverages the enhanced safety aspects (nonvolatility and nonflammability) of solvate ionic liquids is to support the SIL with a polymeric scaffold, creating a composite gel (*i.e.* a solvate ionogel) electrolyte.[10-13] The polymeric scaffold provides structural support to the liquid component in a gel electrolyte via some combination of physical and/or chemical cross-links.[14] Kitazawa *et al.* fabricated solvate ionogels through the self-assembly of an ABA-triblock copolymer consisting of polystyrene and poly(methyl methacrylate) (PMMA) blocks inside a SIL to create a physically cross-linked network.[10] At 10 wt.% copolymer loading, this solvate ionogel demonstrated a room temperature ionic conductivity of ~0.4 mS cm^{-1} and a lithium ion transport number (calculated via NMR spectroscopy-derived ion self-diffusivity values) value of 0.52, although the mechanical stiffness was relatively low (shear modulus ~2 kPa).[10] The effects of varying the SIL-compatible B segment identity on $[Li(G4)]^+$ complex stability in ABA-triblock copolymer-supported solvate

ionogels has also recently been reported.[12] Unemoto and coworkers synthesized quasi-solid-state solvate ionogels using a silica nanoparticle-based scaffold to yield a room temperature ionic conductivity of 0.15 mS cm^{-1} and a lithium ion transport number of 0.53.[15] Recently, our group demonstrated a chemically cross-linked polymer scaffold-based solvate ionogel that leveraged the use of ethylene oxide groups within the polymer network to increase the lithium ion transport number to 0.58 for a 21 vol.% PEGDA-supported ionogel.[13] However, investigators have yet to demonstrate a highly stretchable, self-healable solvate ionogel, which could provide great versatility for the design of next-generation flexible and wearable energy storage devices.

In this work, a novel class of solvate ionogel electrolytes exhibiting widely tunable mechanical properties and high room temperature ionic conductivities has been fabricated via *in situ* UV-initiated free radical (co)polymerization of a fully-zwitterionic (f-ZI) polymer network within the SIL [Li(G4)][TFSI]. Zwitterionic functional group-containing polymer networks have recently been demonstrated to improve the elastic modulus[14] and electrochemical properties (*i.e.* ionic conductivity and t_{Li^+})[16] of various ionogel electrolytes due to favorable zwitterion-zwitterion and zwitterion-ion interactions, respectively. A number of zwitterionic polymers have been reported in the literature for their endowment of unique properties to new materials;[17-22] however, most of the investigations to date have focused on their potential applications in aqueous environments (*e.g.* hydrogels). The molecular structures of the solvate ionogel components used here are shown in **Fig. 1a** and **Fig. 1b**; each solvate ionogel polymer scaffold consists solely of some combination of the zwitterionic monomers 2-methacryloyloxyethyl phosphorylcholine (MPC) and sulfobetaine vinylimidazole (SBVI). Solvate ionogels were synthesized with varying f-ZI polymer contents and compositions, and both compressive/tensile tests and electrochemical measurements were performed. A lithium-ion battery (LIB) containing a f-ZI solvate ionogel

electrolyte has also been successfully fabricated and characterized by galvanostatic charge/discharge cycling. The present results suggest that the cationic species of the SIL interact strongly with the MPC repeat unit functional groups (*i.e.* phosphorylcholine) of the polymer network to facilitate a highly stretchable and self-healing ionogel composite. Meanwhile, the SBVI repeat unit functional groups (*i.e.* sulfobetaine) tend to self-associate, creating a higher degree of physical cross-linking via zwitterionic dipole-dipole interactions that promote a higher elastic modulus. We propose that SIL-MPC favorable interactions facilitate the formation of *dynamic* physical cross-links, which render these unique solvate ionogels capable of self-healing and a high degree of plastic deformation prior to fracture in tensile tests. This investigation demonstrates the highly tunable mechanical properties of a new class of solvate ionogels that can be controlled based on the selection of specific zwitterionic repeat unit(s) in the polymer network, allowing for the rational design of stretchable, mechanically robust, and self-healable gel electrolytes for Li-based energy storage devices.

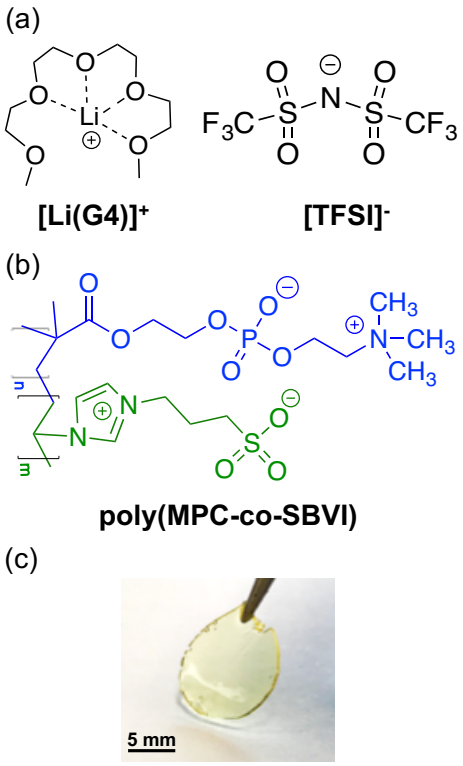

Figure 1. (a) Molecular structures of solvate ionogel components: lithium-tetraglyme complex cation $[Li(G4)]^+$ and bis(trifluoromethylsulfonyl)imide anion $[TFSI]^-$ that comprise the solvate ionic liquid (SIL). (b) Molecular structure of a fully-zwitterionic copolymer scaffold consisting of phosphorylcholine pendant groups (top, blue) from the 2-methacryloyloxyethyl phosphorylcholine (MPC) monomer and sulfobetaine groups (bottom, green) from the sulfobetaine vinylimidazole (SBVI) monomer. (c) Photograph of a representative thin, circular solvate ionogel containing a poly(MPC-co-SBVI) scaffold with a 7:1 MPC:SBVI molar ratio, 20 mol% total polymer content.

Experimental Section

Materials

All materials were used as received and stored in a nitrogen-filled glove box (O_2 < 0.1 ppm) until time of use unless stated otherwise. Tetraglyme (G4), photoinitiator 2-hydroxy-2-methylpropiophenone (HOMPP), lithium bis(trifluoromethylsulfonyl)imide (LiTFSI), and 2-

methacryloyloxyethyl phosphorylcholine (MPC) were purchased from Sigma Aldrich. LiTFSI and MPC were heated *in vacuo* at 70 °C for 24 hours before being placed in a nitrogen-filled glove box and a glass desiccator, respectively. G4 was dried over molecular sieve beads (5Å, Sigma Aldrich) for 48 hours inside a nitrogen-filled glove box. Sulfobetaine vinylimidazole (SBVI) was prepared according to a previous study[23] (see Supporting Information) and dried *in vacuo* at 70 ºC for 24 hours before being placed in a glass desiccator. Lithium foil (0.75 mm thick) was purchased from MTI Corporation (99.9% metals basis) and stored in an argon-filled glove box (H_2O, O_2 < 0.5 ppm). Stainless steel shim (18-8 grade, 0.05 mm thickness) was purchased from McMaster-Carr and cleaned successively in acetone and isopropanol baths via sonication before drying *in vacuo* at 70 ºC and placed in the Ar-filled glove box. The cathode sheet was aluminum foil coated with lithium nickel cobalt manganese oxide, $LiNi_{0.5}Co_{0.2}Mn_{0.3}O_2$ (NCM 5:2:3, 45 μm thickness, 155 mAh g^{-1}), the anode sheet was copper foil coated with CMS graphite (140 μm thickness, 330 mAh g^{-1}); both electrode sheets, as well as *Celgard* separator (25 μm thickness) and coin cell parts (CR2032), were purchased from MTI Corp. and dried *in vacuo* at 70 °C prior to storage in the Ar-filled glove box. A conventional LIB electrolyte, 1.0 M $LiPF_6$ in ethylene carbonate/dimethyl carbonate (EC/DMC, 50/50 v/v) solution, was purchased from Sigma Aldrich.

Solvate Ionogel Synthesis

[Li(G4)][TFSI] was prepared by combining an equimolar mixture of LiTFSI and G4 in a vial and stirred overnight at 70 ºC inside a nitrogen-filled glove box to yield a clear, homogenous liquid. Zwitterionic copolymer-supported solvate ionogels were fabricated by mixing a specified quantity of SBVI and/or MPC into [Li(G4)][TFSI] in a nitrogen-filled glove box at 50 ºC for approximately 1 h until a clear precursor solution was obtained. The molar ratio of SBVI:MPC was varied on a monomeric basis, *i.e.* a poly(MPC-co-SBVI), 3:1 scaffold refers to a solvate

ionogel that was fabricated from a precursor solution having a molar ratio of 3 mol MPC to 1 mol of SBVI in the SIL. Approximately 2 wt.% (based on total monomer content) HOMPP was added to the precursor solution prior to *in situ* UV irradiation at 365 nm (Spectronic Corp., 8 W) within a Teflon-lined mold for 10 min. All precursor solutions and solvate ionogel composites were visually transparent except for those having a polymer scaffold consisting entirely of SBVI (see Fig. S1, Supporting Information).

Electrical Characterization

AC impedance spectroscopy measurements were performed using a VersaSTAT 3 potentiostat with a built-in frequency response analyzer (Princeton Applied Research) over the frequency range of 1 Hz to 100 kHz using a sinusoidal voltage amplitude of 10 mV (0 V DC offset), with all samples located inside the glove box. Solvate ionogel samples were prepared *in situ* within a custom-built Teflon cell array featuring gold-plated electrical probes. The geometrical cell factor used to convert limiting impedance at high frequency to ionic conductivity was determined by prior calibration using three different pure IL electrolytes. Variable temperature impedance spectroscopy measurements were performed by placing samples on a temperature-controlled microscopy stage (Linkam Scientific Instruments, LTS 420) with two thin electrical probes inserted directly into the solvate ionogel (diameter = 6.35 mm, thickness = 3.16 mm). A 15-min holding period was utilized during each temperature step change to allow for thermal equilibration. A best-fit line possessing a R^2 value > 0.99 was implemented for each sample in calculating the activation energy of ionic conductivity (E_a) using the linearized Arrhenius model.

Mechanical Characterization

Compressive testing was performed in free-extension mode using a dynamic mechanical analyzer (RSA3, TA Instruments) in ambient conditions at a rate of 0.01 mm/s to a maximum of

10% strain. The compressive testing samples were cylindrical in shape with an aspect ratio of approximately 2:1 (6.35 mm diameter x 3.16 mm thickness). The compressive elastic modulus of each sample was calculated as the slope of a best-fit line to the stress-strain data between 0–10% strain. Tensile testing was performed at a rate of 0.1 mm/s in ambient conditions. The solvate ionogels for tensile tests were fabricated using a PDMS mold to produce rectangular gels with the dimensions: 40 mm long x 8 mm wide x ~0.5 mm thick. Sample ends were placed between the instrument forceps using sandpaper to prevent slippage; samples were positioned ~5 mm into the forceps on either end, leaving ~30 mm of specimen to undergo tensile strain. Rheological measurements were performed in order to demonstrate the self-healing ability of the solvate ionogels under repeated cycles of high and low shear strains. Tests were carried out with a TA Instruments ARES-LS2 rheometer using stainless steel parallel plates. Samples were cycled at a constant frequency of 1 Hz while switching between 0.1% strain to 200% strain. Each cycle consisted of 100 s between switching the strain value with no rest period in between cycles.

Self-Healing Puncture & Slice Tests

Solvate ionogels were investigated for their ability to self-heal using multiple approaches. A puncture test was performed, consisting of puncturing a cylindrical ionogel (6.35 mm diameter x 3.16 mm thickness) with a metal syringe needle (21 gauge) through the entire gel thickness. For the first slice test, a rectangular specimen (4 cm long x 1 cm wide x 2 mm thick) was fabricated and then sliced in half with a razor blade. Each slice was treated with a different food coloring (Wilton) color for visual clarity. The slices were gently pressed together on top of a glass slide. Following either the puncture or slice traumas, samples were heated on a hotplate at 50 ºC inside a nitrogen-filled glove box for 1 h to observe their ability to self-heal. Self-healing was confirmed by disappearance of the syringe incision and the ability for the sliced sample to be readily handled

as a single piece without breaking apart. In a second slice test, two cylindrical ionogel specimens (6.35 mm diameter x 3.16 mm thickness) were sliced in half diagonally along the direction of their thickness, yielding two equal wedge-shaped pieces for each sample. These pieces were then gently pressed back together, and one sample was allowed to rest at 23 °C for 12 h while the other was heated on a hotplate at 50 C for 1 h. The extent of self-healing was probed by comparing compressive stress-strain data measured before and after slicing/healing for each specimen.

Thermal Characterization

Thermogravimetric analysis (TGA) measurements were carried out with a TA Instruments Q500 Thermogravimetric Analyzer at a heating rate of 10 °C min^{-1} under a nitrogen gas flow of 50 mL min^{-1}. Isothermal hold tests were also performed at 80 ºC for an extended period while the sample mass was recorded. Differential scanning calorimetry (DSC) was performed using a TA Instruments Q100 instrument that was calibrated with indium and sapphire standards. Tests were performed under a N_2 gas flow of 50 mL min^{-1}. Each sample was supercooled first to -80 °C at a rate of 10 °C min^{-1} to prevent crystallization and to better observe any glass transitions during the heating scan. Displayed DSC traces are for the heating scan, measured at a ramp rate of 5 °C min^{-1}. Sample masses were consistently between 3.5–4.5 mg.

Electrochemical Cell Testing

All measurements were performed inside an Ar-filled glove box at room temperature with H_2O and O_2 levels < 0.5 ppm. Solvate ionogel samples of 1.27 cm diameter and ~500 μm thickness were prepared using a PDMS mold and subsequently incorporated into a coin cell (CR2032) inside the Ar-filled glove box. For liquid electrolyte (SIL) tests, a *Celgard* separator was soaked in SIL *in vacuo* at 70 °C overnight. Typically, ~100 μL of additional SIL electrolyte was injected into each CR2032 coin cell prior to assembly in order to fill the entire cell volume and promote

sufficient wetting of the porous electrodes for both solvate ionogel and liquid electrolyte cells. Linear sweep voltammetry experiments were performed using a VersaSTAT 3 potentiostat at a scan rate of 1 mV s^{-1} with Li foil (Cu foil-backed) as the counter electrode and a stainless steel 18-8 disc as the working electrode. For lithium-ion transference number (t_{Li^+}) calculations, the method of Evans et al.[24] was employed for DC polarization/chronoamperometry combined with impedance spectroscopy in a Li|electrolyte|Li symmetrical cell using an applied potential (ΔV) of 80 mV to measure the initial (I_0) and steady-state (I_{SS}) current responses. It should be noted that the initial current was recorded as the first data point measured during the chronoamperometry test. Impedance spectroscopy was performed to measure the initial (R_0) and final (R_{ss}) resistances of the Li metal interface with either the liquid electrolyte or solvate ionogel. The Li-ion transference number was calculated as:

$$t_{Li^+} = \frac{I_{SS}(\Delta V - I_0 \cdot {}_0\Delta}{I_0(\Delta V - I_{SS} \cdot {}_{SS}\Delta} \qquad \text{(Eq. 1)}$$

In order to calculate the Li^+ conductivity (σ_{Li^+}), or the fraction of the total ionic conductivity (σ) that is due to Li^+ motion, the following expression was used:

$$\sigma_{Li^+} = \sigma t_{Li^+} \qquad \text{(Eq. 2)}$$

Galvanostatic charge-discharge measurements of a full LIB cell with the structure graphite|electrolyte|NCM (5:2:3) were carried out at a rate of C/2 in an assembled CR2032 coin cell. A preconditioning cycle at a rate of C/20 was performed prior to extended charge-discharge cycle testing. Cut-off voltages of 4.2 V and 1.7 V were implemented on the charging and discharging tests, respectively. Electrodes (graphite and NCM), *Celgard*, and solvate ionogels were cut into circular discs having a diameter of 1.27 cm and dried in vacuo at 70 °C overnight before being placed in the Ar-filled glove box. The active loadings of the NCM and graphite discs having this diameter were 15.3 mg and 10.1 mg, respectively, which correspond to a cathode

capacity of 2.37 mAh and an anode capacity of 3.33 mAh. Galvanostatic charge-discharge cycling measurements were performed using an eight-channel battery analyzer (MTI Corp.) at a C/2 rate (current density of 0.94 mA cm^{-2}).

Results and Discussion

Room Temperature Ionic Conductivity and Mechanical Characterization of Solvate Ionogels

The properties of ionic conductivity and compressive elastic modulus are typically coupled in the context of liquid-rich ionogel electrolytes;[25] attempts to increase gel stiffness usually result in a reduction in ionic conductivity. Ionic conductivity is determined both by the concentration of all ionic species that can effectively drift in an applied electric field and their mobility (or diffusivity) values, which may be reduced due to the presence of a dense network of cross-links in the scaffold necessary to obtain a useful gel elastic modulus (at least ~1 kPa). Indeed, when the total f-ZI polymer content (maintaining a fixed 3:1 MPC:SBVI molar ratio) is increased from 6.4 mol% (minimum gelation point at this composition) to 25.2 mol% in [Li(G4)][TFSI], the compressive elastic modulus rises from 0.89 kPa to 2.01 MPa, while the room temperature ionic conductivity simultaneously decreases from 1.34 mS cm^{-1} to 0.47 mS cm^{-1} (see Fig. S2, Supporting Information). It should be noted that the measured ionic conductivity of neat SIL is 1.16 mS cm^{-1} (± 0.10 mS cm^{-1}), which indicates that the ionic conductivity of a very liquid-rich solvate ionogel (*i.e.* 93.6 mol% SIL) can approach or even slightly exceed that of the base liquid electrolyte. Importantly, all solvate ionogels are prepared and handled under strictly moisture-free conditions inside an inert atmosphere glove box in order to eliminate any potential plasticizing effect of absorbed water, which would confound these measurements. One way to understand the possibility

of the ionic conductivity of an ionogel exceeding that of its primary liquid component is an increase in the effective fraction of *mobile*, 'dissociated' ions within the highly ion-dense electrolyte due to favorable ion interactions with the scaffold, in spite of the reduced total ion concentration owing to the presence of a neutral scaffold.[14, 25] On the other hand, when the total polymer content is held fixed while varying the molar ratio between the two zwitterionic groups of the f-ZI copolymer scaffold, we observed that solvate ionogel elastic modulus values could be increased over two orders of magnitude while the ionic conductivity remains relatively unchanged. **Figure 2a** displays the room temperature ionic conductivity and compressive elastic modulus values of f-ZI solvate ionogels having a constant 20 mol% zwitterionic copolymer content, varying the molar ratio of MPC:SBVI (*i.e.* varying the SBVI fraction within the scaffold as shown). The room temperature ionic conductivity was observed to increase only slightly, from 0.48 mS cm^{-1} to 0.70 mS cm^{-1} (± 0.05 mS cm^{-1}), for ionogels with a polymer network containing 0% SBVI (*i.e.* poly(MPC)) versus 100% SBVI (*i.e.* poly(SBVI)), respectively. Comparing the two homopolymer-supported solvate ionogel extremes, the compressive elastic modulus was found to increase 100-fold, from 23 kPa for the 0% SBVI sample to 2.3 MPa for the 100% SBVI gel. Notably, the compressive modulus reached a maximum value of 7.3 MPa for a solvate ionogel containing 75% SBVI in the copolymer scaffold (*i.e.* poly(MPC-co-SBVI), 1:3); this gel electrolyte also displayed a high ionic conductivity of 0.67 mS cm^{-1} (Fig. 2a). This is an intriguing behavior, which indicates that despite a notable increase in scaffold cross-link density (inferred via the increased modulus) as the SBVI fraction in the copolymer is increased, the ionic conductivity does not decrease accordingly, but rather, a slight increase is observed. This can be explained by the different roles that the SBVI and MPC units in the copolymer likely play in the SIL environment. While the phosphorylcholine groups of MPC units interact more strongly with the SIL ions (compared to MPC-MPC self-

associations), SBVI groups preferentially self-associate via stronger zwitterionic dipole-dipole interactions; this was also recently observed to be the case for a traditional IL having the [TFSI]$^-$ anion,[26] and was understood to be driven by solubility differences between the two ZI monomers in the IL. In addition, differences in the charge densities of the anionic and cationic groups between these two ZI monomers and/or reversed dipole orientation relative to the polymer backbone may also be important factors in determining their self-assembly behavior.[27,28] Thus, gels containing SBVI-rich copolymer scaffolds tend to promote both higher elastic modulus values (more ZI cross-links) and higher ionic conductivity (reduced polymer-ion attraction), for a fixed total copolymer content.

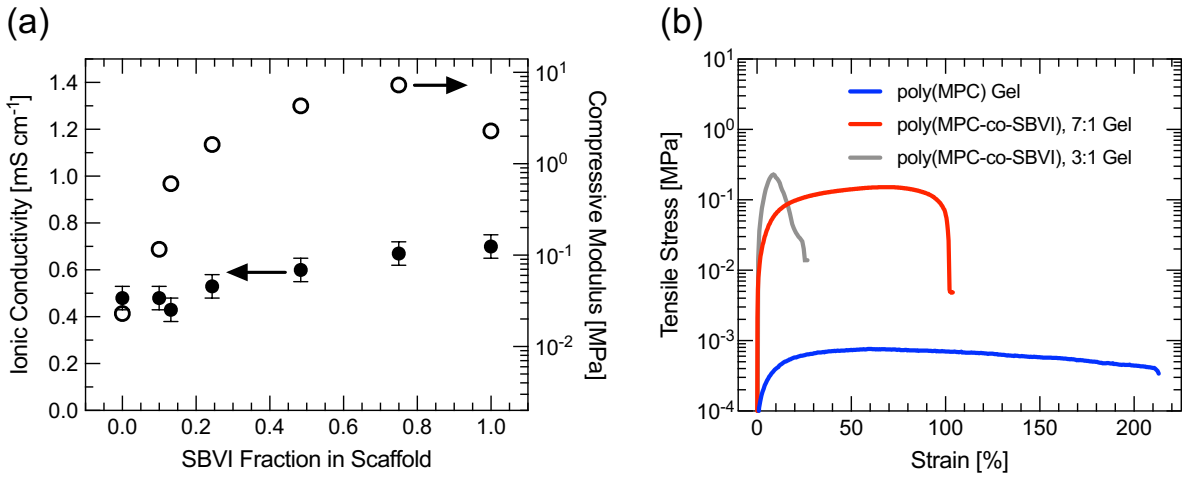

Figure 2. (a) Room temperature ionic conductivity and compressive elastic modulus values of solvate ionogels containing 20 mol% f-ZI (co)polymer scaffolds, varying the SBVI fraction in the MPC/SBVI blend. Error bars for the modulus values are smaller than the size of the points shown. The ionic conductivity of the neat SIL, [Li(G4)][TFSI], is 1.16 ± 0.10 mS cm^{-1}. (b) Tensile stress vs. strain curves for 20 mol% f-ZI solvate ionogels with varying MPC:SBVI molar ratios.

While SBVI-rich scaffolds tend to increase solvate ionogel stiffness, they have also been observed to result in more brittle gel mechanical character for the case of hydrophobic ILs.[26] Therefore, tensile stress-strain measurements were performed on the f-ZI solvate ionogels in order to determine the extent of their stretchability for potential flexible device applications. **Figure 2b** depicts representative tensile stress vs. strain curves measured for three different f-ZI solvate ionogels, all containing 20 mol% (co)polymer scaffolds and varying the molar ratio of MPC:SBVI repeat units. The poly(MPC-co-SBVI)-supported solvate ionogel with a 3:1 MPC:SBVI molar ratio exhibits the most brittle nature of the three, with the sample yielding at 9% strain and displaying an ultimate tensile strength (UTS) of 230 kPa. This sample experiences some plastic deformation and abruptly ruptures with a ~28% strain at failure. The solvate ionogel having a 7:1 MPC:SBVI scaffold ratio (*i.e.* lower SBVI fraction) exhibits a comparable UTS of 151 kPa at 70% strain, and displays a wider plastic deformation phase that begins at 20% strain until failure at ~100% strain. The solvate ionogel containing no SBVI in the zwitterionic network (*i.e.* a poly(MPC) scaffold) displayed the widest plastic deformation phase, extending from 25% strain to 210% strain (see also Fig. S3, Supporting Information) while exhibiting the lowest UTS of only 0.8 kPa. While these f-ZI solvate ionogels all display comparable room temperature ionic conductivity values (Fig. 2a), it is evident that both the compressive and tensile properties of these gel electrolytes can be widely tuned based upon the selected molar ratio of MPC:SBVI. Considering both the compressive and tensile testing results, it appears that SBVI repeat units in the polymer network indeed facilitate strong dipole-dipole cross-links that produce solvate ionogels of a stiffer and more brittle nature; meanwhile, MPC repeat units impart a softer and more stretchable nature to the gels. Previous reports have demonstrated an enhancement in the stretchability of hydrogels with polymer scaffolds containing zwitterionic repeat units[29] and ion-

mediated cross-links (*i.e.* metal ion-polymer coordination).[30] Gel stretchability is generally promoted by weaker, dynamic cross-links that can effectively dissipate energy as the gels are deformed. Here, we hypothesize that dynamic cross-links may be formed between the more highly-solvated/SIL-philic MPC repeat units of these f-ZI solvate ionogels due to the high affinity of MPC for Li^+, as shown in our previous report with a traditional IL-based electrolyte.[16] Additional efforts, including computational modeling of these materials, are ongoing to further test this hypothesis.

Due to the physical (noncovalent) nature of zwitterionic dipole-dipole cross-links, it was also imperative to learn at approximately what elevated temperature the f-ZI solvate ionogels may begin to disassemble, resulting in SIL leakage. The compressive modulus of a poly(MPC-co-SBVI), 9:1 gel was observed to decrease monotonically from 116 kPa at 25 °C to 8.4 kPa at 70 °C (Table S1, Supporting Information) while the gel visually retained its free-standing shape up to a maximum of 80 °C (Fig. S4, Supporting Information), proving its structural integrity over a practical temperature usage range for Li-based batteries. To compare the mechanical properties of f-ZI solvate ionogels in the context of current battery electrolyte technology, a commercial separator, *Celgard* (trilayer polypropylene-polyethylene-polypropylene) was soaked in SIL and subjected to stress-strain testing; the SIL-soaked *Celgard* sample demonstrated a UTS of ~60 MPa with minimal plastic deformation (see Fig. S5, Supporting Information) while abruptly rupturing at ~30% strain, suggesting it to be impractical for next-generation stretchable devices. By comparison, the poly(MPC-co-SBVI), 7:1 solvate ionogel offers greater stretchability and a softer mechanical character that is well-suited to the mechanical requirements of highly bendable/stretchable devices.

Self-Healing Ability

Considering the soft and stretchable nature of the MPC-rich f-ZI solvate ionogels, several tests were conducted to assess the capability of these materials to self-heal after the gel had been mechanically compromised. Some polymeric materials have previously been reported to self-heal with the stimulus of UV light or gentle heating.[31] A self-healable character may be an advantage for any solid electrolytes intended for wearable devices that could experience substantial deformation during their use. First, a 20 mol% poly(MPC-co-SBVI), 7:1 solvate ionogel was punctured with a 22-gauge syringe needle and then placed on a hotplate at 50 ºC for 1 h inside a nitrogen-filled glove box. It was visually observed that the pierced hole completely healed with no evidence of the original puncture (**Fig. 3a**). Next, a rectangular bar-shaped solvate ionogel of the same composition was sliced in half using a razor blade; each half was colored with a different food coloring dye (red, yellow) for visual clarity, and then the two halves were gently pushed back into contact and subsequently placed on a hotplate at 50 ºC for 1 h in the glove box. The original incision line was no longer visible after 1 h, and the healed solvate ionogel could be substantially bent without breaking, verifying a high degree of self-healing within the composite (**Fig. 3b**). Compressive testing of healed solvate ionogels also revealed nearly complete recovery of their original stress-strain responses (Fig. S6, Supporting Information). Finally, in order to investigate the cyclability of the self-healing behavior, shear rheometry measurements were performed on a 20 mol% poly(MPC-co-SBVI), 7:1 solvate ionogel sample. **Figure 3c** displays the storage (G') and loss (G") components of the shear modulus measured at room temperature during repeated alternation of the shear strain from 1% to 200% (frequency of 1 Hz; approximately 100 cycles at each strain before switching). The solvate ionogel exhibited G' and G" values of 216 kPa and 68 kPa, respectively, for the first cycle at 1% shear strain, indicating solid-like viscoelastic behavior (G' > G"). However, the G' value decreased significantly to 55 kPa during the first cycle at 200%

shear strain, while G" remained at 62 kPa, revealing significant disruption of the f-ZI cross-linked network and a liquid-like character. Additional rheological data obtained for this solvate ionogel formulation can be found in the Supporting Information (Fig. S7). As seen in Fig. 3c, after four switches of approximately 100 cycles each between 1% and 200% strain, the ionogel exhibited final G' and G'' values of 220 kPa and 88 kPa at 1 % strain, respectively, confirming the robust nature of the self-healing behavior.

We posit that dynamic zwitterionic cross-links readily broken and reformed between MPC units on different copolymer chains, and interacting closely with the lithium-containing SIL cation $[Li(G4)]^+$, provide the ability for the f-ZI solvate ionogel composite to self-heal. The high mobility of the polymer chains due to the absence of any covalent cross-links allows for the scaffold network to repair itself by forming new ZI physical cross-links, given a sufficient amount of time and/or thermal energy input. A recent investigation by Tang et al. demonstrated the ability of a double-network ionogel to heal at 100 °C, in which the composite featured both thermoreversible physical and dynamic covalent cross-linked networks.[32] The f-ZI solvate ionogels described here are unique because they leverage the assembly of a single network of dynamic *noncovalent* cross-links enabled by zwitterionic functional groups, without the addition of any other cross-link-mediating species.

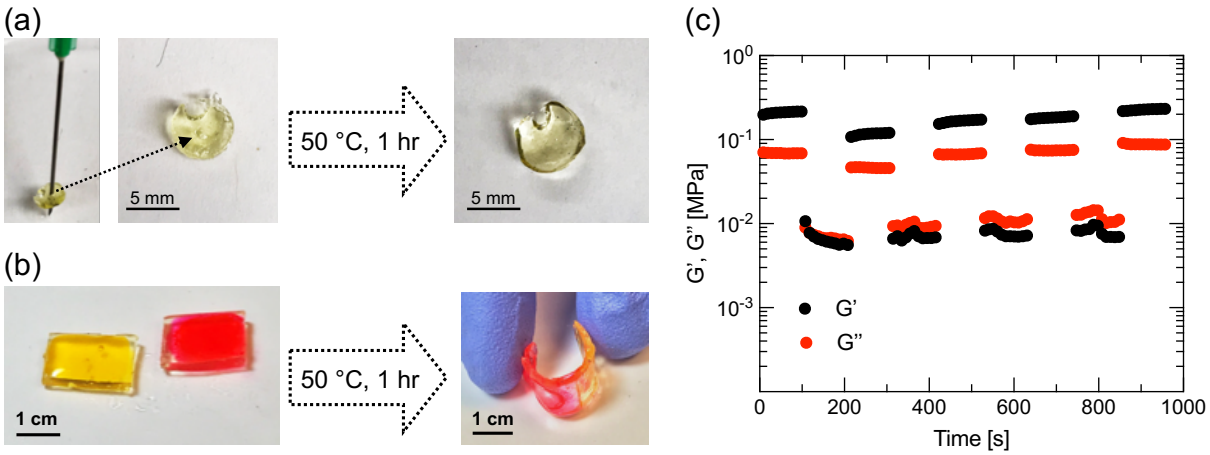

Figure 3. Demonstrations of the self-healing ability of a 20 mol% poly(MPC-co-SBVI), 7:1 solvate ionogel. (a) Photographs showing a puncture test performed with a 22-gauge syringe needle; the hole in the gel was observed to be fully healed after being heated at 50 ºC for 1 h. (b) Photographs showing the self-healing of a rectangular bar-shaped gel initially cut into two pieces, each dyed a different color, then heated at 50 ºC for 1 h. The healed gel could be substantially bent without breaking. (c) Rheological measurements of a solvate ionogel that was alternately subjected to ~100 cycles (frequency = 1 Hz) of 1% shear strain (upper data groupings) and 200% shear strain (lower data groupings) at room temperature, demonstrating repeatable switching between solid-like and liquid-like behaviors.

Thermal Characterization and Temperature Dependence of Ionic Conductivity

The low thermal stability of conventional organic solvent-based battery electrolytes is usually the limiting factor in terms of high temperature battery performance and safety.[33] The SIL [Li(G4)][TFSI] has previously been shown to exhibit high thermal stability, losing less than 5 wt.% at temperatures below 180 °C during a standard thermogravimetric analysis (TGA) heating scan at 10 °C min^{-1}.[13] The primary factor that contributes to the ultralow volatility of

[Li(G4)][TFSI] is the stability of the $[Li(G4)]^+$ complex cation;[6] the presence of any excess tetraglyme would greatly reduce the stability at elevated temperatures due to the volatile nature of pure G4 (see **Figure 4a**). Solvate ionogels containing 20 mol% f-ZI homopolymer networks were observed to exhibit comparable thermal degradation stability to neat SIL at temperatures below ~300°C, above which the zwitterionic polymer networks begin to degrade, as shown in Fig. 4b. This indicates that the f-ZI polymer scaffolds studied here do not limit the thermal stability of this new class of solvate ionogels. The TGA data also verify the stability of the solvate cation $[Li(G4)]^+$ in the presence of both the SBVI and MPC zwitterionic functional groups, suggesting that these groups do not interact with the cation strongly enough to dissociate Li^+ from G4, as the solvate ionogels did not exhibit any substantial weight loss below ~150 ºC compared to the SIL. Raman spectroscopy (see Fig. S8, Supporting Information) further confirms the unaltered nature of the $[Li(G4)]^+$ complex within the f-ZI solvate ionogels. The advantages of higher thermal stability and ultralow volatility of the SIL and a f-ZI solvate ionogel compared to a conventional liquid LIB electrolyte (1 M $LiPF_6$ in ethylene carbonate/dimethyl carbonate) were demonstrated via an isothermal hold test at 80 ºC (see Fig. S9, Supporting Information) that revealed < 1 wt.% loss after 3 h for both SIL and f-ZI solvate ionogel samples, compared to 93 wt.% loss for the standard LIB electrolyte.

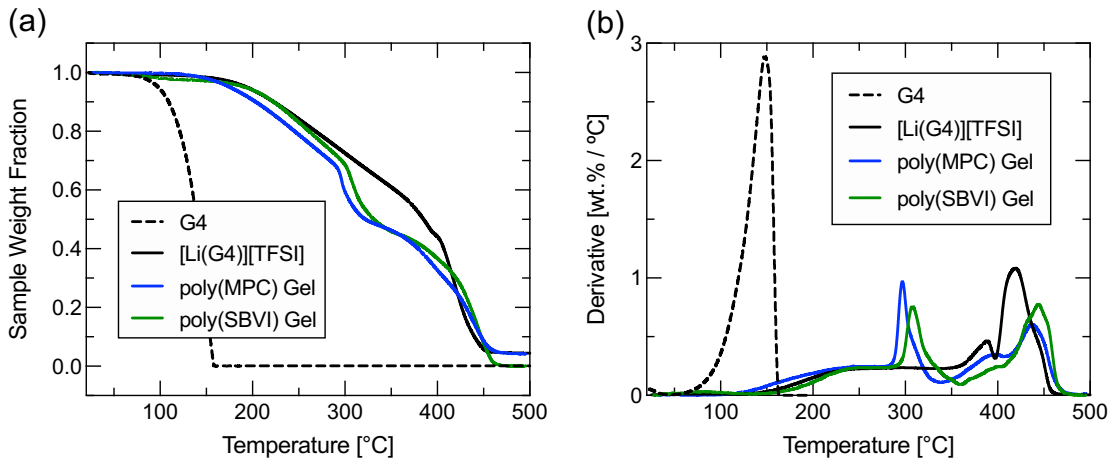

Figure 4. (a) Thermogravimetric analysis scans and (b) their first derivatives measured for tetraglyme (G4), neat SIL ([Li(G4)][TFSI]), a 20 mol% poly(MPC) f-ZI solvate ionogel, and a 20 mol% poly(SBVI) f-ZI solvate ionogel. The heating rate was 10 ºC min^{-1}.

Temperature-dependent ionic conductivity measurements were performed within the range of 23 ºC to 80 ºC using three f-ZI solvate ionogel compositions and the neat SIL, as shown in **Figure 5**. The data were found to obey the simple Arrhenius model across this temperature range, which may be expected since the glass transition temperature of the SIL is much lower, at -61 ºC.[5] No thermal events were observed between 23 °C and 80 °C for either a representative f-ZI solvate ionogel or the neat SIL according to differential scanning calorimetry scans (see Fig. S10, Supporting Information). Comparing the activation energy of ionic conductivity (E_a) values of the f-ZI solvate ionogels to that of the neat SIL, which were calculated from the slopes of the best-fit lines displayed in **Figure 5**, is a means by which one can probe the relative extent of interactions between the different polymer scaffolds and the mobile ionic species of the SIL. Generally, a higher activation energy of ionic conductivity in an ionogel compared to that of its base liquid electrolyte signifies a higher energetic barrier that needs to be overcome in order for ionic species

to be transported in an applied electrostatic potential gradient. This parameter can thus be an indication of the extent of coordination/attraction between ionic species and the polymer network to the degree that ionic motion is affected.[25] While the E_a value of the neat SIL was measured to be 20.8 kJ mol^{-1}, the E_a values of the three 20 mol% f-ZI polymer-supported solvate ionogels were found to be: 25.2 kJ mol^{-1} for the poly(MPC) gel, 23.6 kJ mol^{-1} for the poly(MPC-co-SBVI), 1:1 gel, and 21.0 kJ mol^{-1} for the poly(SBVI) gel (all values ± 0.5 kJ mol^{-1}). Accordingly, the E_a values inversely follow the room temperature ionic conductivity trend for these solvate ionogel formulations (see Fig. 2a). This is consistent with the understanding of stronger polymer-ion interactions in MPC-rich solvate ionogels, compared to fewer polymer-ion attractive interactions (but more ZI polymer-polymer interactions) in SBVI-rich solvate ionogels. A similar scenario occurs in the case of f-ZI copolymer-supported ionogels in a non-lithium-containing hydrophobic ionic liquid,[26] which underscores the importance of understanding the implications of zwitterion chemistry selection when designing these types of materials.

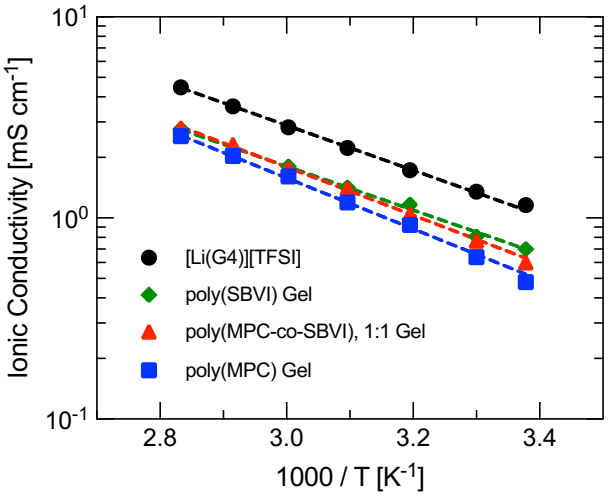

Figure 5. Temperature dependence of ionic conductivity for [Li(G4)][TFSI] and three f-ZI solvate ionogels containing 20 mol% total polymer scaffold with varying MPC:SBVI molar ratios.

Another manifestation of the clear difference between ZI functional group-ion interactions for MPC versus SBVI moieties in these solvate ionogels is revealed upon measuring the Li-ion transference number (t_{Li^+}) via chronoamperometry/DC polarization.[24] The t_{Li^+} values for the same four electrolytes examined in Fig. 5 are summarized in **Table 1**, along with their E_a and E_M values, room temperature ionic conductivity (σ) and Li^+ conductivity (σ_{Li^+}, here, the contribution to the total conductivity due solely to $[Li(G4)]^+$ species) values. While the E_a values increase and the σ values decrease with a greater fraction of MPC in the f-ZI scaffold as discussed previously, the t_{Li^+} values of the solvate ionogels are observed to increase substantially as the MPC fraction is increased. Compared to the neat SIL, which displays a t_{Li^+} value of 0.12 (notably different compared to its lithium transport number derived via self-diffusion measurements of ~0.5),[10,13] the f-ZI solvate ionogel t_{Li^+} values are seen to increase from 0.10 for the poly(SBVI)-supported gel to 0.60 for the poly(MPC)-supported gel, with the poly(MPC-co-SBVI), 1:1 gel value (0.42) intermediate between these two extremes (see also Table S2, Supporting Information). The substantial increase in t_{Li^+} for MPC-rich f-ZI solvate ionogels may be attributed to the advantageous attractive interaction between the MPC units of the polymer network and the $[Li(G4)]^+$ SIL ions that promotes $[Li(G4)]^+/[TFSI]^-$ ion pair dissociation and/or a reduction in ion clustering. Interestingly, the relative increase seen in t_{Li^+} for MPC-rich f-ZI solvate ionogels compared to the base SIL value appears to be even greater than what was recently observed for the case of f-ZI ionogels featuring a 1 M LiTFSI/ionic liquid solution electrolyte.[16] This may be attributable to the higher effective concentration of Li^+ present in the SIL (2.8 M) and/or the strongly chelated nature of its $[Li(G4)]^+$ complex cation, although further investigation is required to fully elucidate the differences between the two systems. The Li^+ conductivity (σ_{Li^+}) values of the three f-ZI solvate ionogel formulations shown in Table 1 highlight the nonlinear nature of the

increase in t_{Li^+} obtained with increasing MPC fraction in the scaffold; the poly(MPC-co-SBVI), 1:1 gel indicates the possibility of achieving a f-ZI copolymer-supported solvate ionogel that yields a higher compressive modulus than either homopolymer-supported gel and also exhibits a nearly two-fold increase in σ_{Li^+} compared to the neat SIL. Taking into account both the greater gel stiffness that can be realized by increasing the SBVI fraction in the scaffold and the improvements in Li^+ conductivity, stretchability, and a self-healing capability obtained at large MPC fractions, it is clear that these f-ZI solvate ionogels can provide exquisite versatility for designing solid-state lithium-ion electrolytes to meet the demands of next-generation energy storage devices.

Table 1. Activation energy of ionic conductivity (E_a), compressive elastic modulus (E_M), Li-ion transference number measured via chronoamperometry (t_{Li^+}), room temperature ionic conductivity (σ), and Li^+ conductivity (σ_{Li^+}) of SIL versus three f-ZI solvate ionogel formulations (each containing 20 mol% total polymer scaffold).

Sample	E_a [kJ mol^{-1}]	E_M [kPa]	t_{Li^+}	σ [mS cm^{-1}]	σ_{Li^+} [mS cm^{-1}]
[Li(G4)][TFSI]	20.8	-	0.12	1.18	0.14
poly(SBVI) Gel	21.0	2300	0.10	0.70	0.07
poly(MPC-co-SBVI), 1:1 Gel	23.6	4300	0.42	0.60	0.25
poly(MPC) Gel	25.2	23	0.60	0.48	0.29

Electrochemical Stability and Battery Demonstrations

For Li-based battery applications, it is critical to determine the anodic and cathodic voltage stability limits of any electrolyte in order to minimize parasitic side reactions and decomposition of the electrolyte during the charging/discharging processes. **Figure 6a** displays linear sweep voltammetry (LSV) data collected for [Li(G4)][TFSI] and a representative f-ZI solvate ionogel, a 20 mol% poly(MPC-co-SBVI), 3:1 gel, using a stainless steel working electrode and a scan rate of 1 mV s^{-1}. This solvate ionogel formulation was selected for electrochemical cell testing due to its balance of: suitable stiffness for handling, moderate stretchability, and a high t_{Li^+} value (0.51, see below). As seen in Fig. 6a, both the neat SIL and the f-ZI solvate ionogel demonstrate high anodic stability up to ~5.4 V vs. Li/Li^+ (*i.e.* current density below 0.1 mA cm^{-2}). The cathodic stability around 0 V vs. Li/Li^+ is displayed in **Figure 6b**. Minimal breakdown of electrolyte is observed prior to the onset of lithium plating (-0.4 V vs. Li/Li^+), indicating good reductive stability of the f-ZI polymer, $[Li(G4)]^+$, and $[TFSI]^-$ species (see Fig. S11, Supporting Information for 2nd

cycle data). Considering both anodic and cathodic stability, the f-ZI solvate ionogel is seen to possess a stability window > 5 V, making such materials potential candidates both for high voltage cathodes and Li metal anodes (see Fig. S12, Supporting Information for open-circuit stability in symmetric Li metal cells). **Figure 6c** shows the chronoamperometry responses of neat SIL and the f-ZI solvate ionogel, which were used to determine their t_{Li^+} values (0.12 and 0.51, respectively). Galvanostatic charge-discharge measurements were performed over 100 cycles on graphite|electrolyte|NCM (5:2:3) full-cell LIB configurations using a high rate of C/2 (**Fig. 6d**). Although the initial discharge capacity of each cell approached the theoretical capacity limited by the NCM cathode (155 mAh g^{-1}), a significant capacity fade is observed for both the neat SIL and the f-ZI solvate ionogel during the first 50 cycles, which may be attributed to the high C-rate and non-optimization of the cut-off voltage range, which may be important for NCM cathodes.[34] In spite of this, the f-ZI solvate ionogel appears to perform comparably to and even slightly better than the neat SIL in terms of capacity retention up to 100 cycles. A more in-depth investigation of the cut-off voltage range and strategies to improve the Coulombic efficiency (~90% for the f-ZI solvate ionogel cell) will be pursued in future studies. Notably, the f-ZI solvate ionogel was also successfully incorporated into a functional Li metal anode cell that could be cycled at least 100 times (Fig. S13, Supporting Information). Thus, the poly(MPC-co-SBVI), 3:1 solvate ionogel proved to be electrochemically viable for both lithium-ion and Li metal-based cells, exhibiting a high Li-ion transference number that makes it an intriguing candidate for further development in the battery arena.

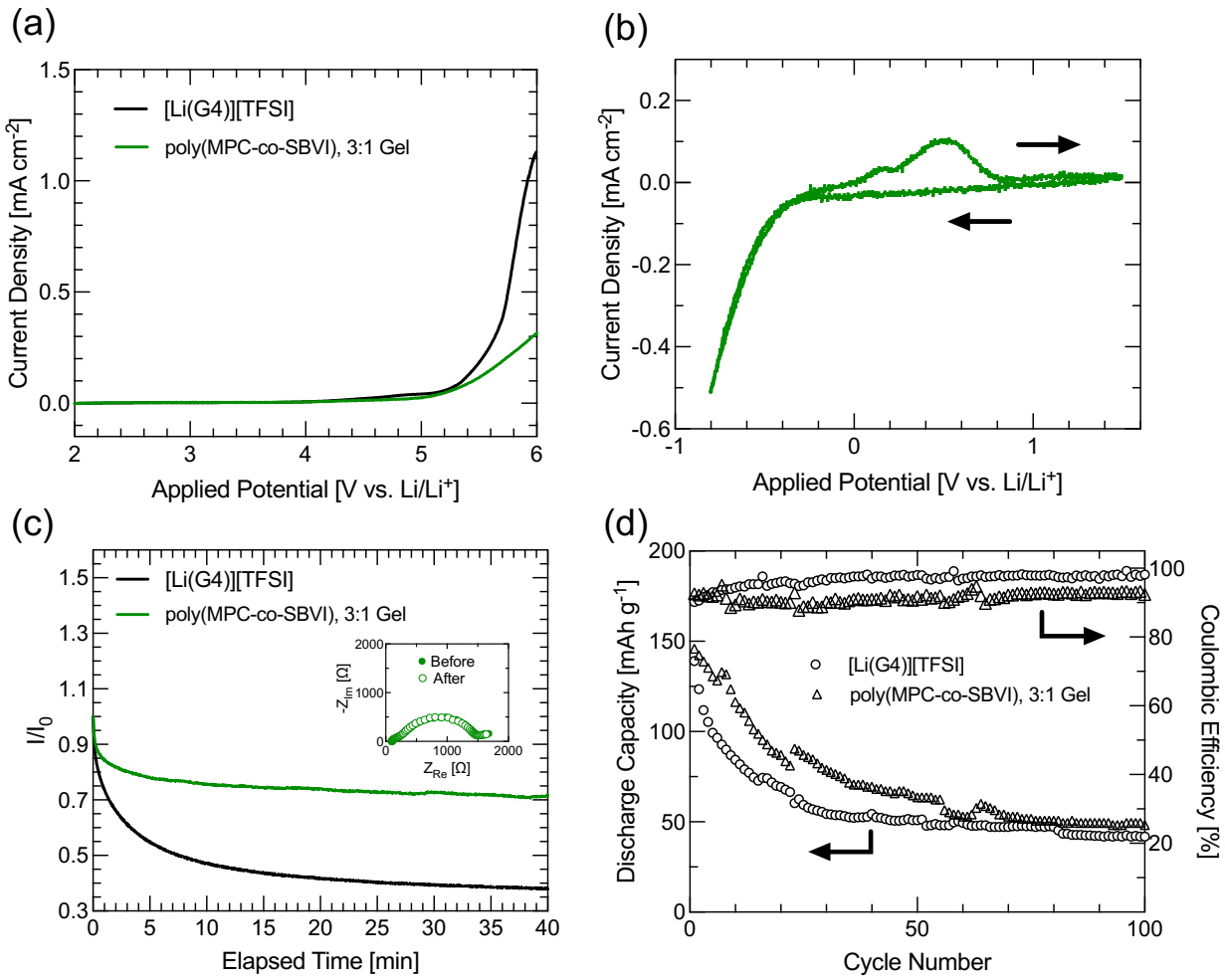

Figure 6. (a) Linear sweep voltammograms (1 mV s^{-1}) of neat SIL and a 20 mol% poly(MPC-co-SBVI), 3:1 solvate ionogel. (b) Cathodic cyclic voltammogram (1 mV s^{-1}) obtained near 0 V vs. Li/Li^+ for a 20 mol% poly(MPC-co-SBVI), 3:1 solvate ionogel. (c) Chronoamperometry responses to DC polarization at 80 mV for neat SIL and a 20 mol% poly(MPC-co-SBVI), 3:1 solvate ionogel; inset displays the cell impedance frequency response obtained before and after polarization for the f-ZI solvate ionogel. (d) Discharge capacity and Coulombic efficiency profiles over 100 cycles for graphite|SIL|NCM and graphite|f-ZI solvate ionogel|NCM cells at a C/2 rate; cut-off voltages were 4.2 V and 1.7 V.

Conclusions

The *in situ* synthesis of fully-zwitterionic (co)polymer scaffolds within the solvate ionic liquid [Li(G4)][TFSI] facilitated the creation of a new class of Li^+-conducting solvate ionogel electrolytes that demonstrated good room temperature Li^+ conductivity, high stretchability, and a capacity to self-heal. Varying the molar ratio of the two zwitterionic monomers (MPC and SBVI) for a fixed total 20 mol% polymer content enabled tunability of the solvate ionogel compressive elastic moduli over two orders of magnitude; meanwhile, the room temperature ionic conductivity remained relatively unchanged (0.48 to 0.70 mS cm^{-1}). The different extent of interaction between SBVI/MPC and the SIL cations versus zwitterionic group self-association was determined to be the primary factor responsible for the wide range of mechanical properties that could be realized. MPC-rich f-ZI solvate ionogels possessed scaffolds that could form dynamic physical cross-links in the SIL that enabled plastic deformation up to 200% strain and rapid self-healing at 50 ºC. Li-ion transference number values were also found to substantially increase for greater MPC fractions in the polymer scaffold. A 20 mol% poly(MPC-co-SBVI), 3:1 solvate ionogel demonstrated an electrochemical stability window > 5 V and could be successfully discharged and charged at a C/2 rate for at least 100 cycles in a graphite|solvate ionogel|NCM LIB cell. Therefore, f-ZI solvate ionogel electrolytes may be promising materials for realizing safer solid-state Li-based batteries with good flexibility/stretchability, which also allow one to fine-tune their properties based on the specific zwitterion chemistries employed.

Acknowledgements

The authors gratefully acknowledge Morgan Taylor for assistance with the initial f-ZI solvate ionogel synthetic screening. This research was performed with financial support from the Massachusetts Clean Energy Center and from the National Science Foundation (CBET-1802729).

Supporting Information

SBVI synthesis details; photographs of solvate ionogels; additional ionic conductivity and compressive elastic modulus data; additional tensile/compressive stress-strain data; gel shear rheometry and self-healing data; Raman spectra; thermal characterization data; additional cyclic voltammetry, impedance spectroscopy and chronoamperometry data; galvanostatic charge/discharge cycling data for a lithium metal battery with a f-ZI solvate ionogel electrolyte (PDF)

Notes

One of the authors (A. J. D'Angelo) is the founder of Lithio Storage, Inc., a start-up company seeking to develop safer battery electrolytes similar to those described in this work.

References

(1) Le Bideau, J.; Viau, L.; Vioux, A. Ionogels, Ionic Liquid Based Hybrid Materials. *Chem. Soc. Rev.* **2011**, *40*, 907-925.

(2) Armand, M.; Endres, F.; MacFarlane, D. R.; Ohno, H.; Scrosati, B. Ionic-Liquid Materials for the Electrochemical Challenges of the Future. *Nat. Mater.* **2009**, *8*, 621-629.

(3) Fernicola, A.; Croce, F.; Scrosati, B.; Watanabe, T.; Ohno, H. LiTFSI-BEPyTFSI as an Improved Ionic Liquid Electrolyte for Rechargeable Lithium Batteries. *J. Power Sources* **2007**, *174*, 342-348.

(4) Frömling, T.; Kunze, M.; Schönhoff, M.; Sundermeyer, J.; Roling, B. Enhanced Lithium Transference Numbers in Ionic Liquid Electrolytes. *J. Phys. Chem. B* **2008**, *112*, 12985-12990.

(5) Pappenfus, T. M.; Henderson, W. A.; Owens, B. B.; Mann, K. R.; Smyrl, W. H. Complexes of Lithium Imide Salts with Tetraglyme and Their Polyelectrolyte Composite Materials. *J. Electrochem. Soc.* **2004**, *151*, A209-A215.

(6) Mandai, T.; Yoshida, K.; Ueno, K.; Dokko, K.; Watanabe, M. Criteria for Solvate Ionic Liquids. *Phys. Chem. Chem. Phys.* **2014**, *16*, 8761-8772.

(7) Ueno, K.; Yoshida, K.; Tsuchiya, M.; Tachikawa, N.; Dokko, K.; Watanabe, M. Glyme–Lithium Salt Equimolar Molten Mixtures: Concentrated Solutions or Solvate Ionic Liquids? *J. Phys. Chem. B* **2012**, *116*, 11323-11331.

(8) Aguilera, L.; Xiong, S.; Scheers, J.; Matic, A. A Structural Study of LiTFSI–Tetraglyme Mixtures: from Diluted Solutions to Solvated Ionic Liquids. *J. Mol. Liq.* **2015**, *210*, 238-242.

(9) Liu, W.; Song, M. S.; Kong, B.; Cui, Y. Flexible and Stretchable Energy Storage: Recent Advances and Future Perspectives. *Adv. Mater.* **2017**, *29*, 1603436.

(10) Kitazawa, Y.; Iwata, K.; Imaizumi, S.; Ahn, H.; Kim, S. Y.; Ueno, K.; Park, M. J.; Watanabe, M. Gelation of Solvate Ionic Liquid by Self-Assembly of Block Copolymer and Characterization as Polymer Electrolyte. *Macromolecules* **2014**, *47*, 6009-6016.

(11) Kido, R.; Ueno, K.; Iwata, K.; Kitazawa, Y.; Imaizumi, S.; Mandai, T.; Dokko, K.; Watanabe, M. Li^+ Ion Transport in Polymer Electrolytes Based on a Glyme-Li Salt Solvate Ionic Liquid. *Electrochim. Acta* **2015**, *175*, 5-12.

(12) Kitazawa, Y.; Iwata, K.; Kido, R.; Imaizumi, S.; Tsuzuki, S.; Shinoda, W.; Ueno, K.; Mandai, T.; Kokubo, H.; Dokko, K.; Watanabe, M. Polymer Electrolytes Containing Solvate Ionic Liquids: A New Approach to Achieve High Ionic Conductivity, Thermal Stability, and a Wide Potential Window. *Chem. Mater.* **2018**, *30*, 252-261.

(13) D'Angelo, A. J.; Panzer, M. J. Enhanced Lithium Ion Transport in Poly(ethylene glycol) Diacrylate-Supported Solvate Ionogel Electrolytes via Chemically Cross-linked Ethylene Oxide Pathways. *J. Phys. Chem. B* **2017**, *121*, 890-895.

(14) Lind, F.; Rebollar, L.; Bengani-Lutz, P.; Asatekin, A.; Panzer, M. J. Zwitterion-Containing Ionogel Electrolytes. *Chem. Mater.* **2016**, *28*, 8480-8483.

(15) Unemoto, A.; Matsuo, T.; Ogawa, H.; Gambe, Y.; Honma, I. Development of All-Solid-State Lithium Battery Using Quasi-Solidified Tetraglyme–Lithium Bis(trifluoromethanesulfonyl)amide–Fumed Silica Nano-Composites as Electrolytes. *J. Power Sources* **2013**, *244*, 354-362.

(16) D'Angelo, A. J.; Panzer, M. J. Decoupling the Ionic Conductivity and Elastic Modulus of Gel Electrolytes: Fully Zwitterionic Copolymer Scaffolds in Lithium Salt/Ionic Liquid Solutions. *Adv. Energy Mater.* **2018**, *8*, 1801646.

(17) Lowe, A. B.; McCormick, C. L. Synthesis and Solution Properties of Zwitterionic Polymers. *Chem. Rev.* **2002**, *102*, 4177-4189.

(18) Carr, L. R.; Zhou, Y.; Krause, J. E.; Xue, H.; Jiang, S. Uniform Zwitterionic Polymer Hydrogels with a Nonfouling and Functionalizable Crosslinker Using Photopolymerization. *Biomaterials* **2011**, *32*, 6893-6899.

(19) Han, D.; Letteri, R.; Chan-Seng, D.; Emrick, T.; Tu, H. Examination of Zwitterionic Polymers and Gels Subjected to Mechanical Constraints. *Polymer* **2013**, *54*, 2887-2894.

(20) Hu, G.; Emrick, T. Functional Choline Phosphate Polymers. *J. Am. Chem. Soc.* **2016**, *138*, 1828-1831.

(21) Peng, X.; Liu, H.; Yin, Q.; Wu, J.; Chen, P.; Guangzhao, Z.; Liu, G.; Wu, C.; Xie, Y. A Zwitterionic Gel Electrolyte for Efficient Solid-State Supercapacitors. *Nat. Commun.* **2016**, *7*, 11782.

(22) Ye, L.; Zhang, Y.; Wang, Q.; Zhou, X.; Yang, B.; Ji, F.; Dong, D.; Gao, L.; Cui, Y.; Yao, F. Physical Cross-Linking Starch-Based Zwitterionic Hydrogel Exhibiting Excellent Biocompatibility, Protein Resistance, and Biodegradability. *ACS Appl. Mater. Interfaces* **2016**, *8*, 15710-15723.

(23) Carr, L.; Cheng, G.; Xue, H.; Jiang, S. Engineering the Polymer Backbone to Strengthen Nonfouling Sulfobetaine Hydrogels. *Langmuir* **2010**, *26*, 14793-14798.

(24) Evans, J.; Vincent, C. A.; Bruce, P. G. Electrochemical Measurement of Transference Numbers in Polymer Electrolytes. *Polymer* **1987**, *28*, 2324-2328.

(25) D'Angelo, A. J.; Grimes, J. J.; Panzer, M. J. Deciphering Physical Versus Chemical Contributions to the Ionic Conductivity of Functionalized Poly(methacrylate)-Based Ionogel Electrolytes. *J. Phys. Chem. B* **2015**, *119*, 14959-14969.

(26) Taylor, M. E.; Panzer, M. J. Fully-Zwitterionic Polymer-Supported Ionogel Electrolytes Featuring a Hydrophobic Ionic Liquid. *J. Phys. Chem. B* **2018**, *122*, 8469-8476.

(27) Shao, Q.; Mi, L.; Han, X.; Bai, T.; Liu, S.; Li, Y.; Jiang, S. Differences in Cationic and Anionic Charge Densities Dictate Zwitterionic Associations and Stimuli Responses. *J. Phys. Chem. B* **2014**, *118*, 6956-6962.

(28) Shao, Q.; Jiang, S. Molecular Understanding and Design of Zwitterionic Materials. *Adv. Mater.* **2015**, *27*, 15-26.

(29) Ning, J.; Li, G.; Haraguchi, K. Synthesis of Highly Stretchable, Mechanically Tough, Zwitterionic Sulfobetaine Nanocomposite Gels with Controlled Thermosensitivities. *Macromolecules* **2013**, *46*, 5317-5328.

(30) Sun, J.-Y.; Zhao, X.; Illeperuma, W. R. K.; Chaudhuri, O.; Oh, K. H.; Mooney, D. J.; Vlassak, J. J.; Suo, Z. Highly Stretchable and Tough Hydrogels. *Nature* **2012**, *489*, 133-136.

(31) Burnworth, M.; Tang, L.; Kumpfer, J. R.; Duncan, A. J.; Beyer, F. L.; Fiore, G. L.; Rowan, S. J.; Weder, C. Optically Healable Supramolecular Polymers. *Nature* **2011**, *472*, 334-337.

(32) Tang, Z.; Lyu, X.; Xiao, A.; Shen, Z.; Fan, X. High-Performance Double-Network Ion Gels with Fast Thermal Healing Capability via Dynamic Covalent Bonds. *Chem. Mater.* **2018**, *30*, 7752-7759.

(33) Maleki, H.; Deng, G.; Anani, A.; Howard, J. Thermal Stability Studies of Li-Ion Cells and Components. *J. Electrochem. Soc.* **1999**, *146*, 3224-3229.

(34) Zheng, H.; Sun, Q.; Liu, G.; Song, X.; Battaglia, V. S. Correlation Between Dissolution Behavior and Electrochemical Cycling Performance for $LiNi_{1/3}Co_{1/3}Mn_{1/3}O_2$-Based Cells. *J. Power Sources* **2012**, *207*, 134-140.

Table of Contents Image (TOC)